

Influence of Current Pulsing on Mechanical Properties and Microstructure of Tungsten Inert Gas (TIG) Welded AISI 304L Austenite Stainless Steel Joints

¹V Ganesan*, ²K Shanmugam, ³V Balasubramanian

¹P.G Student, ²Associate Professor, ³Professor, Centre for Materials Joining & Research (CEMAJOR), Department of Manufacturing Engineering, Annamalai University, Annamalai Nagar-608002

*Email: classicganes99@gmail.com

DOI : 10.22486/iwj/2019/v52/i4/186788

ABSTRACT

The Austenitic Stainless Steels (ASS) are probably the most widely used materials in stainless steels, category AISI 304L is an important grade of the ASS, which is commonly used in many of important industries such as containers of transporting chemicals, oil refinery, nuclear reactor tanks, dairy industries, and textile industries. Currently, 304L Austenitic stainless steel sheets are used as fuel tanks in Armour Fighting Vehicle (AFV). These tanks are fabricated by conventional Tungsten Inert Gas (TIG) welding process. In conventional welding, fusion zones typically exhibit coarse columnar grains because of the prevailing thermal conditions during weld metal solidification. This often results in inferior weld mechanical properties. Interpulse Tungsten Inert Gas (IPTIG) welding is a new variant of conventional Tungsten Inert Gas (TIG) welding process. This process offers many advantages over conventional TIG welding process such as narrow heat affected zone, deeper penetration compared to Constant Current TIG (CCTIG) and Pulsed Current TIG (PCTIG) welding processes. The present investigation was carried out to understand the effect of arc pulsing technique on cross sectional weld bead profile, micro hardness, microstructure and the tensile properties of welded joints. It is found that IPTIG welded joints showed superior mechanical properties compared to CCTIG and PCTIG joints, and this is mainly due to formation of finer grains in the fusion zone, caused by the combined effect of arc constriction and pulsating action.

Keywords: Tungsten Inert Gas; Austenitic stainless steel; Interpulse TIG Welding; Tensile properties; Microstructure.

1.0 INTRODUCTION

AISI 304L low carbon content austenitic stainless steel (ASS) is one of the most versatile and widely used material due to its superior strength, toughness and corrosion resistance in a wide variety of applications which does not limit to aerospace, automotive, nuclear and thermal power plants, pressure vessels, petroleum refineries, cryogenic environments, pulp and paper industries, acidic medium, food processing, kitchen appliances [1-3]. Majority of the fabricators prefer AISI 304L due to its excellent weldability with less metallurgical problems in the fusion welding techniques. Heat input is one of the

influencing factors that affect the quality of the weldments. Many researchers addressed that the welding of AISI 304L must be carried out using an optimal heat input to avoid the deformation of the weldments and also to avoid the metallurgical effects. Giridharan et al. [4] reported that heat input has a significant impact on the bead geometry, metallurgical, mechanical and corrosion resistance properties of the welds. Similarly, Karunakaran [5] reported that the rate of heat input during welding followed by the nature of cooling has a strong influence on the grain size and phase formation. As recommended by Martin [6], the maximum heat input that

can be employed for joining AISI 304L should not exceed 1.5 kJ/mm.

Yousefieh et al. [7] observed that excessive heat input during welding resulted in the formation of brittle inter metallic phases and/or the formation of coarse columnar grains which resulted in poor weld mechanical properties and adversely affected the corrosion resistance. Kou et al. [8] found that current pulsing is an effective technique to control the heat input and helps in grain refining of the weld fusion zones. Several researchers reported the accrued benefits obtained on employing Pulsed Current Gas Tungsten Arc Welding (PCGTAW) welding that includes efficient use of arc energy, decrease in wastage of heat by conduction through base metal and thus reduced heat affected zone. Further, various researchers reported the beneficial effect of current pulsing which normally result in the refined grain structure both in the weld and weld interface. This shall be attributed to the thermal cycle in which temperature goes to a peak value followed by rapid cooling in these zones [9]. Hence a more controlled bead profile can be expected on employing pulsed current than the continuous current mode. It is also reported that the successful welds are usually quantified by obtaining higher penetration and lower bead width. Thus it is desirable to have lower aspect ratio (AR) in a weld, which is obtained by controlled heat input, thereby resulting in good weld properties [10]. It is also suggested that the welding conditions should be controlled to obtain slower cooling rate for adequate austenite formation and fast enough

to prevent deleterious precipitation. Similarly the selection of peak current (I_p) and base current (I_b) must be adequate enough to obtain desired bead contour, bead penetration and stable arc as reported by Balasubramanian et al. [11].

From the literature review, it is understood that lot of research works have been carried out on pulsed current TIG (PCTIG) welding of stainless steel. However the published information on Interpulse TIG (IPTIG) welding of stainless steel are very scant. Hence the present investigation was carried out to evaluate mechanical and microstructural features of IPTIG welded AISI 304L ASS and compare the characteristics with CCTIG and PCTIG welded joints.

2.0 EXPERIMENTAL PROCEDURE

The rolled sheets of 2 mm thickness, 304L alloy were cut to the required dimensions (150*100*2 mm) by machining process. The chemical composition and mechanical properties of the base metal are presented in **Table 1 (a-b)**.

A square butt joint configuration, was prepared to fabricate the joints. The sheets were mechanically and chemically cleaned by acetone before welding to eliminate surface contamination. The welding conditions and optimized process parameters presented in **Table 2** were used to fabricate the joints. The initial joint configuration was obtained by securing the sheet in position using mechanical clamps. The direction of welding was normal to the rolling direction.

Table 1 : (a) Chemical Composition (wt%) of base metal

Material	C	Mn	Cr	Ni	P	Si	N	S	Fe
AISI 304L	0.03	2.11	18	8.6	0.045	0.75	0.10	0.03	Bal

Table 1 : (b) Mechanical properties of base metal

Material	Tensile strength (MPa)	0.2% Yield Strength (MPa)	Elongation in 25 mm gauge length (%)	Micro hardness (HV _{0.2})
AISI 304L	636	280	107	264

Table 2 : Optimized welding parameters and conditions used to fabricate the joints

Process	CCTIG	PCTIG	DSTIG	DPTIG
Tungsten electrode diameter (mm)	1.2	1.2	1.2	1.2
Voltage (volts)	9	9	9	9
Main Current (amps)	90	95	75	80
Delta Current (amps)	-	-	50	60
Base Current (amps)	-	60	-	55
Delta Frequency (kHz)	-	-	20	20
Welding Speed (mm/min)	70	70	70	70
Shielding Gas (100% Argon)	Argon	Argon	Argon	Argon
Gas Flow Rate (lit/min)	10	10	10	10
Heat Input (J/mm)	694.23	597.85	491.78	482.14

3.0 RESULTS AND DISCUSSION

3.1 Macrostructure

The macrographs shown in **Table 3** clearly reveal the difference in weld bead geometry of the four different welding modes. CCTIG welded joint possesses wider Fusion zone (FZ) and heat affected zone (HAZ) compared to the other welding processes. DPTIG and DSTIG welded joint possesses narrow weld FZ and narrow HAZ compared to the other welding processes. The sample welded using PCTIG process shows the FZ of intermediate width between CCTIG and IPTIG processes.

3.2 Microstructure

The optical micrograph of base metal is presented in **Fig. 1**. Optical micrograph of weld zone fusion and HAZ for different welding modes are presented in **Table 4**. It is observed from these optical micrographs that as heat input increases the dendrite size and inter-dendritic spacing in the weld metal also increase. This dendrite size variation can be attributed to the fact that at low heat input, cooling rate is relatively higher due to which steep thermal gradients are established in the weld metal, which in turn allow lesser time for the dendrites to grow, whereas at high heat input, cooling rate is slow which provides sufficient time for the dendrites to grow farther into the fusion zone.

Table 3 : Macrostructure and bead geometry of welding joints

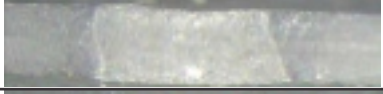
Joint type	Cross section	Depth of Penetration (mm)	Width of Bead (mm)	Fusion Zone Area (mm ²)
CCTIG		2	5.862	9.636
PCTIG		2	4.564	7.934
DSTIG		2	3.828	6.843
DPTIG		2	2.831	6.493



Fig. 1 : Optical micrograph of base metal

Table 4 : Optical micrographs of welded joints

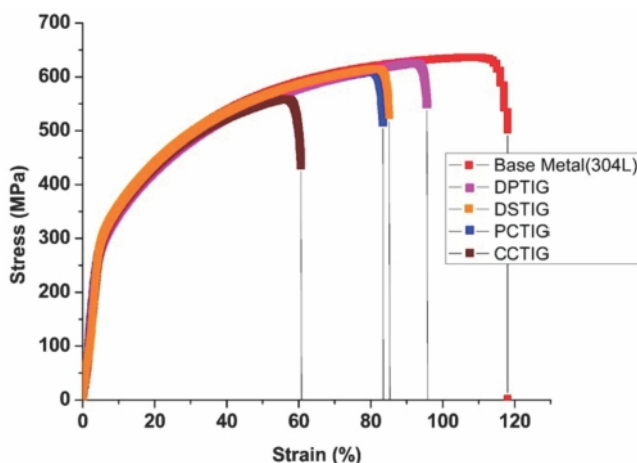
Joint type	Interface	Fusion Zone	Heat Affected Zone
CCTIG	<p>Optical micrograph of the interface for CCTIG. It shows a fusion boundary (FB) indicated by a white arrow, a heat-affected zone (HAZ) to the right, and a fusion zone (FZ) at the bottom left. A scale bar of 200µm is present in the bottom right.</p>	<p>Optical micrograph of the fusion zone for CCTIG, showing a fine, granular, and somewhat uniform microstructure. A scale bar of 200µm is present in the bottom right.</p>	<p>Optical micrograph of the heat-affected zone for CCTIG, showing a coarse, elongated grain structure. A scale bar of 200µm is present in the bottom right.</p>
PCTIG	<p>Optical micrograph of the interface for PCTIG. It shows a fusion boundary (FB) indicated by a white arrow, a heat-affected zone (HAZ) to the left, and a fusion zone (FZ) to the right. A scale bar of 200µm is present in the bottom right.</p>	<p>Optical micrograph of the fusion zone for PCTIG, showing a fine, granular, and somewhat uniform microstructure. A scale bar of 200µm is present in the bottom right.</p>	<p>Optical micrograph of the heat-affected zone for PCTIG, showing a coarse, elongated grain structure. A scale bar of 200µm is present in the bottom right.</p>
DSTIG	<p>Optical micrograph of the interface for DSTIG. It shows a fusion boundary (FB) indicated by a white arrow, a heat-affected zone (HAZ) to the right, and a fusion zone (FZ) at the bottom left. A scale bar of 200µm is present in the bottom right.</p>	<p>Optical micrograph of the fusion zone for DSTIG, showing a fine, granular, and somewhat uniform microstructure. A scale bar of 200µm is present in the bottom right.</p>	<p>Optical micrograph of the heat-affected zone for DSTIG, showing a coarse, elongated grain structure. A scale bar of 200µm is present in the bottom right.</p>
DPTIG	<p>Optical micrograph of the interface for DPTIG. It shows a fusion boundary (FB) indicated by a white arrow, a heat-affected zone (HAZ) to the left, and a fusion zone (FZ) to the right. A scale bar of 200µm is present in the bottom right.</p>	<p>Optical micrograph of the fusion zone for DPTIG, showing a fine, granular, and somewhat uniform microstructure. A scale bar of 200µm is present in the bottom right.</p>	<p>Optical micrograph of the heat-affected zone for DPTIG, showing a coarse, elongated grain structure. A scale bar of 200µm is present in the bottom right.</p>

Table 5 : Transverse tensile properties of welded joints

Joint Type	0.2% Yield strength (MPa)	Tensile strength (MPa)	Joint Efficiency (%)	Elongation in 25 mm gauge length (%)	Notch tensile strength (MPa)	Notch strength ratio	Failure Location
CCTIG	275	559	87.00	60.4	711	1.27	Weld
PCTIG	290	610	95.91	83.2	688	1.12	Weld
DSTIG	346	615	96.00	84.9	707	1.14	Weld
DPTIG	270	626	98.00	95.4	725	1.15	Weld

3.3 Tensile properties

The transverse tensile properties of all the joints were evaluated and presented in **Table 5**. The tensile results show that maximum tensile strength of 626 MPa and 615 MPa are exhibited by the joints made using DSTIG and DPTIG process respectively. PCTIG welded joints showed a tensile strength of 610 MPa. The minimum tensile strength of 559 MPa was yielded by CCTIG joints. The microstructural details of the weld metal in terms of dendrite size and cell spacing, which indicates that high tensile strength and ductility is possessed by the joints at low heat input, process are DPTIG and DSTIG which can be attributed to smaller dendrite sizes and lesser inter-dendritic spacing in the fusion zone. Relatively lower tensile strength and ductility is possessed by the joints with long dendrite sizes and large inter-dendritic spacing in the fusion zone of the joint welded using high heat input process CCTIG. Further it is found that all the tensile specimens fractured in the weld metal. Tensile test was carried out on the similar weldments obtained from arc pulsing techniques are shown

**Fig.2 : Strain-Stress Curves**

in **Fig. 2** which indicates that base metal in all the joints possessed higher tensile strength than the weld metal and thus joint efficiencies of 98%, 96%, 95% and 87% were achieved for DPTIG, DSTIG, PCTIG and CCTIG process respectively.

3.4 Microhardness

Microhardness measurements were taken in the transverse direction i.e. perpendicular to the base plate surface shown in **Fig. 3**. The micro hardness near the top of the weld bead surface is high and as the centre of the fusion/weld zone is approached by the indenter it gradually reduces, which is due to the fact that cooling rate is relatively higher at the top of the weld bead surface than at the centre of the weld metal. From the figure, it is observed that as the indenter traverses outwards parallel to the base plate surface from the centre of the weld/fusion zone towards the fusion boundary, micro hardness increases from 205.5 to 228.8 VHN for DSTIG and DPTIG process, 194.0–210.2 VHN for PGTIG process and 181.1–197.4 VHN for CCTIG process. High hardness as possessed by the fusion boundary zone (FBZ) in all the joints can be attributed to the presence of partially unmelted grains at the fusion boundary which are partially adopted as nuclei by the new precipitating phase of the weld metal during the solidification stage. After reaching this peak value micro hardness shows a decreasing trend in the HAZ. In all the joints, HAZ area adjacent to the fusion boundary was coarse grained HAZ (CGHAZ) which possessed low hardness whereas the HAZ area adjacent to the base metal was fine grained HAZ (FGHAZ) which possessed high hardness. The reason for this trend of micro hardness in the HAZ of all the joints is that the area adjacent to the weld/fusion zone experiences relatively slow cooling rate and hence has coarse grained microstructure, whereas the area adjoining the base metal undergoes high cooling rate due to steeper thermal gradients and consequently has fine grained microstructure. In general it is

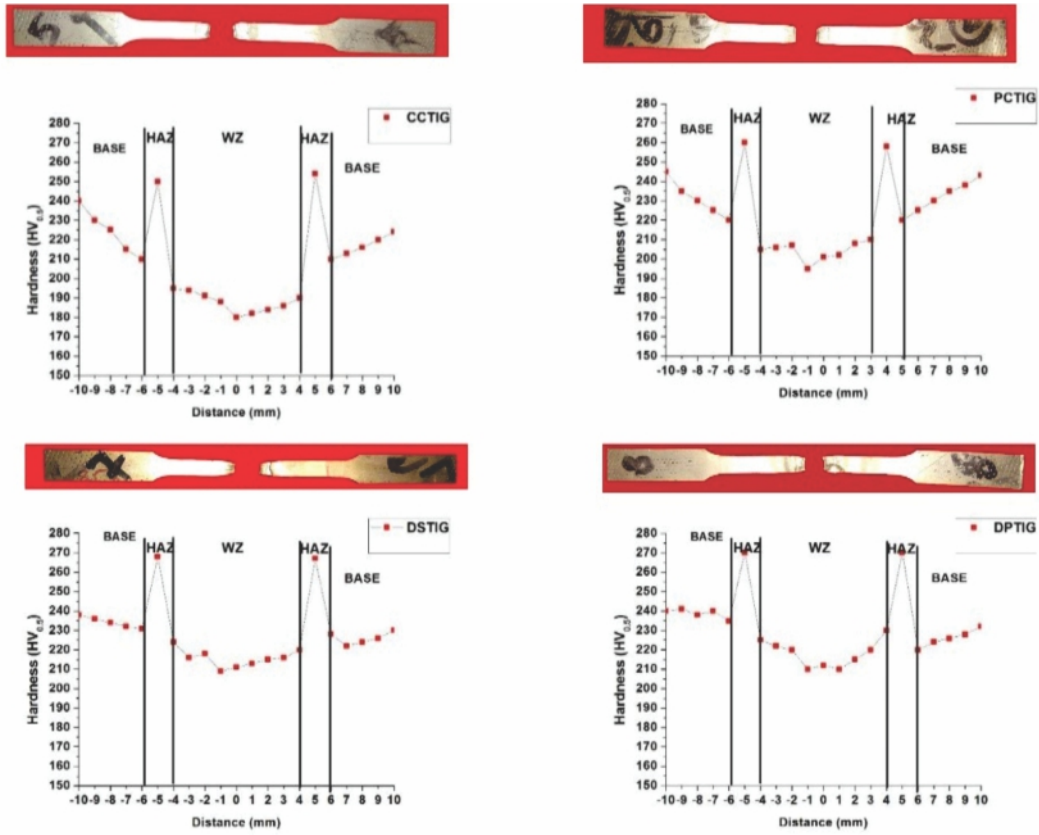


Fig. 3 : Microhardness survey across weld cross-section

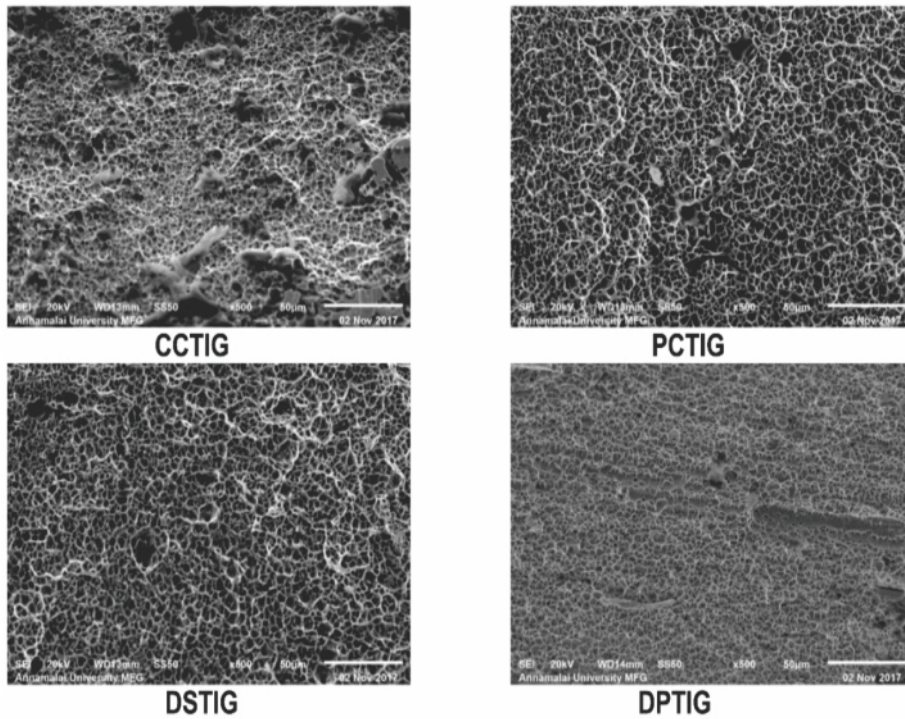


Fig. 4 : Fractographs of tensile specimen

observed from these micro hardness studies that hardness follows an increasing trend in the order of weld metal, HAZ, unaffected base metal and fusion boundary for all the joints made at different processes. It is also observed that there is significant grain coarsening in the HAZ of all the joints.

3.5 Fracture surface analysis

The fractured surfaces of the tensile tested specimens of parent metal and welded joints were analyzed using a scanning electron microscope. The fractographs of tensile specimens are displayed in **Fig. 4**. The modes of failure of the tensile tested parent metal and welded joints are ductile with acceptable plastic deformation and are evident from the fracture location and fractured surface. No brittle cleavage fracture was found in any of the tensile tested fractographs presented at high magnification. However, an appreciable difference in fracture pattern was found. Fine and secondary dimples are the key features of superior tensile strength of DPTIG and DSTIG joint compared to CCTIG, PCTIG and parent metal. The elongated cavities and coarse dimples suggesting localized slip which in turn results in more ductility without reducing the tensile strength of DPTIG joint.

4.0 CONCLUSIONS

The present work addresses on the weldability, microstructure and mechanical properties of AISI 304L using arc pulsing techniques. The summary of conclusions drawn from the present investigation are given as follows:

- (i) Macrostructure clearly shows that interpluse TIG (IPTIG) welding process resulted in narrow fusion zone, and narrow HAZ compared to the PCTIG and CCTIG weld processes.
- (ii) The tensile strength of IPTIG welded joints were 11% higher and shows superior strength when compared to PCTIG and CCTIG weld processes.
- (iii) It is found that dendrite size is smaller in IPTIG welded Joints compared to CCTIG and PCTIG welded joints and this is mainly due to the formation very fine grains in the fusion zone.

REFERENCES

- [1] Viswanathan R and Bakker W (2001); Materials for ultra supercritical coal power plants - boiler materials: part 1, J Mater Eng Perform, 10, pp.81-95.

- [2] Baddoo NR (2008); Stainless steel in construction - a review of research, applications, challenges and opportunities. J of Constructional Steel Research, 64, pp. 1199-06.
- [3] Lippold JC and Koteki DJ (2005); Welding Metallurgy and Weldability of Stainless steels 2nd ed. New Jersey: John Wiley & Sons.
- [4] Giridharan PK and Murugan N (2009); Optimization of pulsed GTA welding process parameters for the welding of AISI 304L stainless steel sheets. Int J Adv Manuf Technol, 40, pp. 478-489.
- [5] Karunakaran N (2012); Effect of pulsed current on temperature distribution, weld profiles and characteristics of GTA welded stainless steel joints. Int J Engineering and Technology, 2, pp.1908-1916.
- [6] Martin L (2014); The Avesta welding manual-practice and products for stainless steel welding. Avesta welding AB, Sweden. www.kskct.cz/images/materialy/en/avesta/.pdf
- [7] Yousefieh M, Shamanian M and Saatchi A (2011); Influence of heat input in pulsed current GTAW process on microstructure and corrosion resistance of duplex stainless steel welds. J. Iron and Steel Research International, 18(9), pp.65-69.
- [8] Kou S and Le Y (1986); Nucleation mechanism and grain refining of weld metal. Welding Journal, 65, pp. 305-313.
- [9] Farahani F, Shamanian F and Ashrafizadeh A (2012); Comparative study on direct and pulsed current gas tungsten arc welding of Alloy 617. AMAE Int J Manufacturing and Material Science, 02 (01), pp.1-6.
- [10] Yousefieh M, Shamanian M and Arghavan AR (2012); Analysis of design of experiments methodology for optimization of pulsed current GTAW process parameters for ultimate tensile strength of UNS S32760 welds. Metallogr Microstruct Anal, 1, pp. 85-91.
- [11] Balasubramanian M, Jayabalan V and Balasubramanian V (2010); Effect of process parameters of pulsed current tungsten inert gas welding on weld pool geometry of titanium welds. Acta Metallurgica. Sinica. (English Letters), 23(4), pp.312-320.